

# A H<sub>2</sub>O<sub>2</sub>-Responsive Theranostic Probe for Endothelial Injury Imaging and Protection

Cheng-Kun Wang, Juan Cheng, Xing-Guang Liang, Chao Tan, Quan Jiang, Yong-Zhou Hu, Ying-Mei Lu, Kohji Fukunaga, Feng Han and Xin Li

## Table of Contents

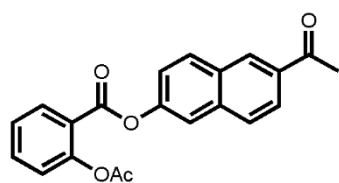
<b>Synthesis and Characterization of AP1-AP4</b> .....	S2
<b>Supplementary Figures</b>	
Figure S1.....	S4
Figure S2.....	S4
Figure S3.....	S5
Figure S4.....	S5
Figure S5.....	S6
Figure S6.....	S6
Figure S7.....	S7
Figure S8.....	S7
Figure S9.....	S8
Figure S10.....	S8
Figure S11.....	S9
Figure S12.....	S9
Figure S13.....	S10
Figure S14.....	S10
Figure S15.....	S10
Figure S16.....	S11
Figure S17.....	S11
Figure S18.....	S12
Figure S19.....	S12
Figure S20.....	S13
Figure S21.....	S14
Figure S22.....	S15
Figure S23.....	S15
Figure S24.....	S16
Figure S25.....	S16
Figure S26.....	S16
<b>NMR traces of AP</b> .....	S17

## Synthesis and characterization of AP1-AP4

### General procedures

To a stirred solution of aspirin (2.0 eq) in CH<sub>2</sub>Cl<sub>2</sub> at 0°C was added HOBT (1.5 eq) and EDC•HCl (1.5 eq). After 20 min, the fluorophore (1.0 eq) and *N,N*-diisopropylethylamine (2.5 eq) were added subsequently and the resulting mixture was stirred at ambient temperature and monitored by thin-layer chromatography analysis. After the disappearance of the fluorophore, H<sub>2</sub>O was added to quench the reaction and the mixture was diluted with CH<sub>2</sub>Cl<sub>2</sub>. The biphasic mixture was then transferred to a separatory funnel and the organic layer was washed sequentially with H<sub>2</sub>O and brine, dried over anhydrous Na<sub>2</sub>SO<sub>4</sub>, filtered, and concentrated under reduced pressure. The remaining residue was purified by flash column chromatography (SiO<sub>2</sub>) to give the product.

### Characterization



AP1

White solid (87% yield)

**M.p.:** 139.4-140.2 °C

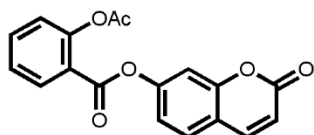
**R<sub>f</sub>** = 0.42 (5:1, petroleum ether:EtOAc).

**<sup>1</sup>H NMR (500 MHz, CDCl<sub>3</sub>, δ):** 8.49 (s, 1H), 8.29 (d, *J* = 8.0, 1H), 8.08 (d, *J* = 8.5 Hz, 1H), 8.04 (d, *J* = 9.0 Hz, 1H), 7.89 (d, *J* = 8.5 Hz, 1H), 7.70 (s, 1H), 7.68 (d, *J* = 8.0 Hz, 1H), 7.44 – 7.40 (m, 2H), 7.22 (d, *J* = 8.0 Hz, 1H), 2.73 (d, *J* = 1.0 Hz, 3H), 2.32 (d, *J* = 1.5 Hz, 3H).

**<sup>13</sup>C NMR (126 MHz, CDCl<sub>3</sub>, δ):** 197.94, 169.85, 162.99, 151.44, 150.37, 136.31, 135.00, 134.67, 132.37, 131.43, 130.80, 130.05, 128.36, 126.40, 124.91, 124.25, 122.43, 122.33, 118.97, 26.80, 21.15.

**IR (KBr, cm<sup>-1</sup>):** 3442, 1676, 1362, 1249, 1142, 902, 745.

**ESI-HRMS (*m/z*):** [M+H]<sup>+</sup> calc'd. for C<sub>21</sub>H<sub>17</sub>O<sub>5</sub>: 349.1076; found 349.1079.



AP2

White solid (79% yield)

**M.p.:** 153.9-155 °C

**R<sub>f</sub>** = 0.52 (4:1, petroleum ether:EtOAc).

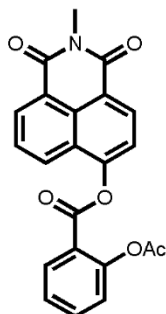
**<sup>1</sup>H NMR (500 MHz, CDCl<sub>3</sub>, δ):** 8.23 (dd, *J* = 8.0, 1.5 Hz, 1H), 7.72 (d, *J* = 10.0 Hz, 1H), 7.70 (dt, *J* = 7.8, 1.5 Hz, 1H), 7.55 (d, *J* = 8.5 Hz, 1H), 7.43 (td, *J* = 7.5, 1.0 Hz, 1H), 7.22 (d, *J* = 2.5 Hz, 1H), 7.21 (dd, *J* = 8.0, 1.0 Hz, 1H), 7.16 (dd, *J* = 8.5, 2.0 Hz, 1H), 6.43 (d, *J* = 10.0 Hz,

1H) 2.32 (s, 3H).

<sup>13</sup>C NMR (126 MHz, CDCl<sub>3</sub>, δ): 169.75, 162.42, 160.38, 154.94, 153.21, 151.53, 142.93, 135.24, 132.32, 128.86, 126.43, 124.31, 122.03, 118.68, 117.09, 116.43, 110.83, 21.13.

IR (KBr, cm<sup>-1</sup>): 3431, 1740, 1512, 1483, 1401, 1244, 1048, 915, 754.

ESI-HRMS (*m/z*): [M+H]<sup>+</sup> calc'd. for C<sub>18</sub>H<sub>13</sub>O<sub>6</sub>: 325.0712; found 325.0729.



AP3

White solid (44% yield)

M.p.: 181.6-183.3 °C

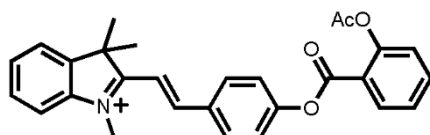
R<sub>f</sub> = 0.40 (5:1, petroleum ether:EtOAc).

<sup>1</sup>H NMR (500 MHz, CDCl<sub>3</sub>, δ): 8.67-8.64 (m, 2H), 8.39 (dd, *J* = 8.0, 1.5 Hz, 1H), 8.31 (dd, *J* = 8.5, 1.0 Hz, 1H), 7.80-7.77 (m, 1H), 7.76 (td, *J* = 7.8, 1.5 Hz, 1H), 7.64 (d, *J* = 8.0 Hz, 1H), 7.50 (dt, *J* = 7.5, 1.0 Hz, 1H), 7.27 (dd, *J* = 8.0, 1.0 Hz, 1H), 3.58 (s, 3H), 2.26 (s, 3H).

<sup>13</sup>C NMR (126 MHz, CDCl<sub>3</sub>, δ): 169.80, 164.43, 163.89, 162.32, 151.76, 151.67, 135.60, 132.38, 131.94, 131.92, 129.48, 128.02, 127.63, 126.62, 125.55, 124.54, 123.05, 121.78, 120.82, 119.88, 27.22, 21.11.

IR (KBr, cm<sup>-1</sup>): 3438, 1755, 1660, 1452, 1234, 1148, 1077, 917, 780.

ESI-HRMS (*m/z*): [M+H]<sup>+</sup> calc'd. for C<sub>22</sub>H<sub>16</sub>NO<sub>6</sub>: 390.0978; found 390.0980.



AP4

Yellow solid (64% yield)

M.p.: 228.9-231.2 °C

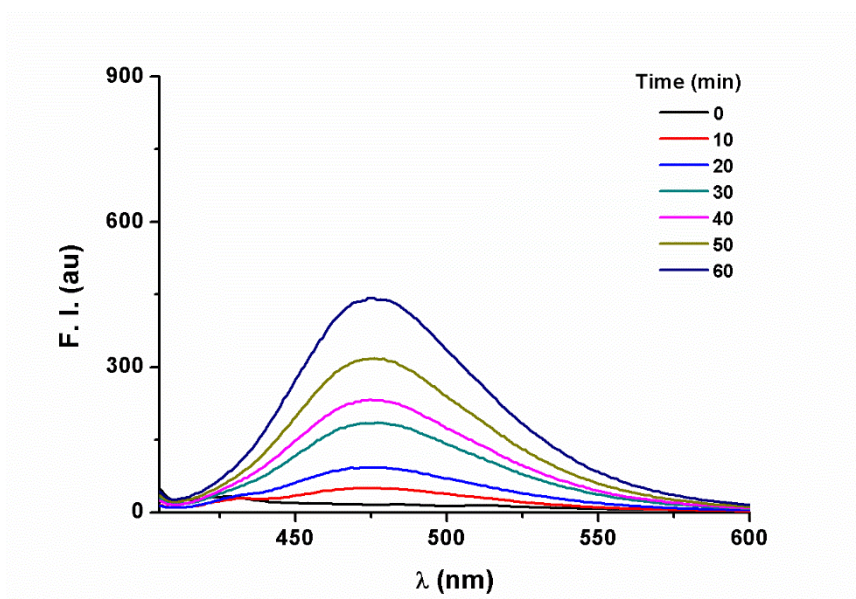
R<sub>f</sub> = 0.40 (10:1, dichloromethane:MeOH).

<sup>1</sup>H NMR (500 MHz, CDCl<sub>3</sub>, δ): 8.26 (s, 1H), 8.25 (d, *J* = 15 Hz, 2H), 8.21 (dd, *J* = 7.5, 1.5 Hz, 1H), 7.84 (d, *J* = 16 Hz, 1H), 7.69-7.64 (m, 2H), 7.60-7.55 (m, 3H), 7.43 (dt, *J* = 7.8, 1.0 Hz, 1H), 7.36 (d, *J* = 8.5 Hz, 2H), 7.20 (dd, *J* = 8.0, 0.5 Hz, 1H), 4.47 (s, 3H), 2.31 (s, 3H), 1.87 (s, 6H), 1.63 (s, 3H).

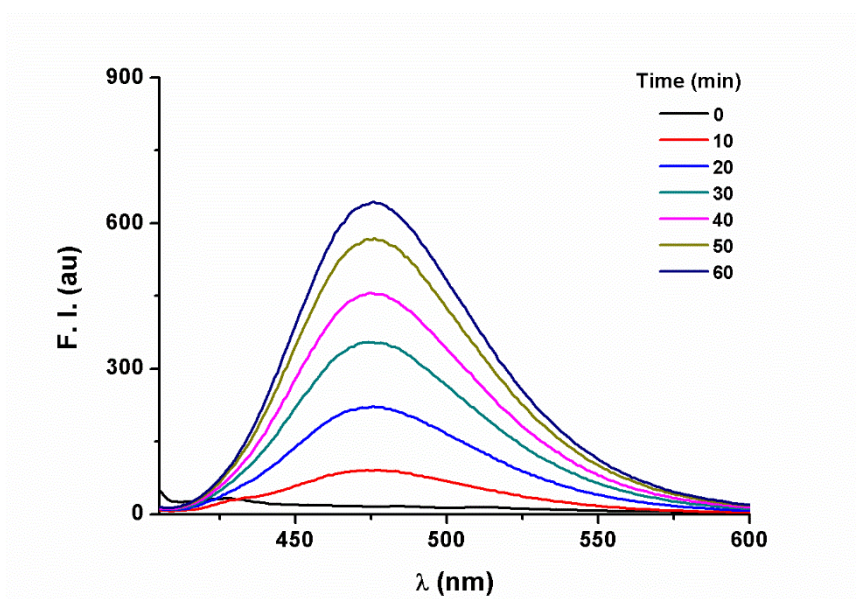
<sup>13</sup>C NMR (126 MHz, CDCl<sub>3</sub>, δ): 182.73, 169.82, 162.44, 154.95, 153.19, 151.42, 143.14, 141.65, 135.16, 132.98, 132.98, 132.36, 131.78, 130.31, 129.90, 126.46, 124.27, 123.09, 123.09, 122.73, 122.19, 115.26, 113.71, 52.88, 37.56, 26.90, 26.90, 21.18.

IR (KBr, cm<sup>-1</sup>): 3451, 1752, 1534, 1402, 1213, 1123, 1014, 916, 760.

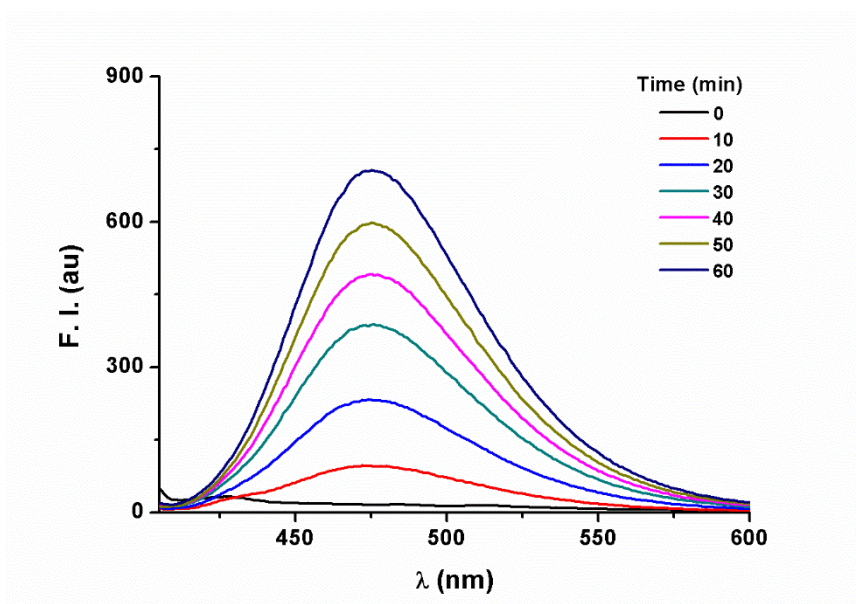
ESI-HRMS (*m/z*): [M+H]<sup>+</sup> calc'd. for C<sub>28</sub>H<sub>26</sub>NO<sub>4</sub><sup>+</sup>: 441.1935; found 441.1937.



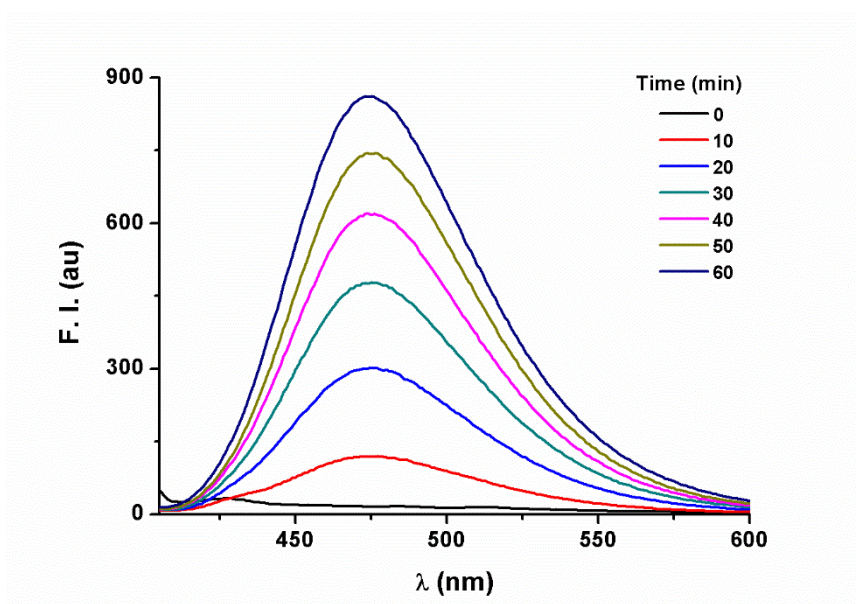
**Figure S1.** Fluorescence response of AP (10  $\mu\text{M}$ ) towards  $\text{H}_2\text{O}_2$  (100  $\mu\text{M}$ ) as time lapsed. Spectra were taken in PBS (pH 7.4, 100 mM) at 37  $^\circ\text{C}$ .



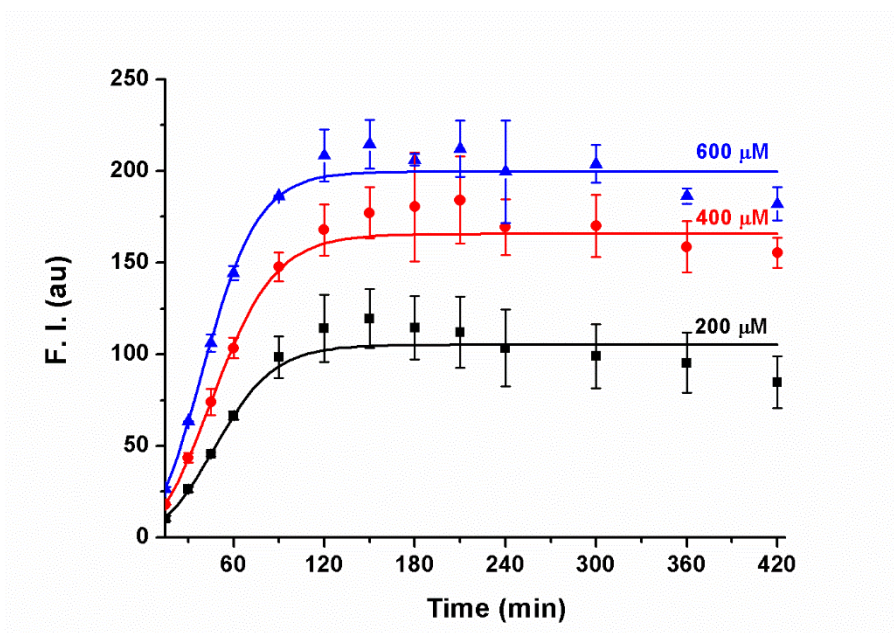
**Figure S2.** Fluorescence response of AP (10  $\mu\text{M}$ ) towards  $\text{H}_2\text{O}_2$  (300  $\mu\text{M}$ ) as time lapsed. Spectra were taken in PBS (pH 7.4, 100 mM) at 37  $^\circ\text{C}$ .



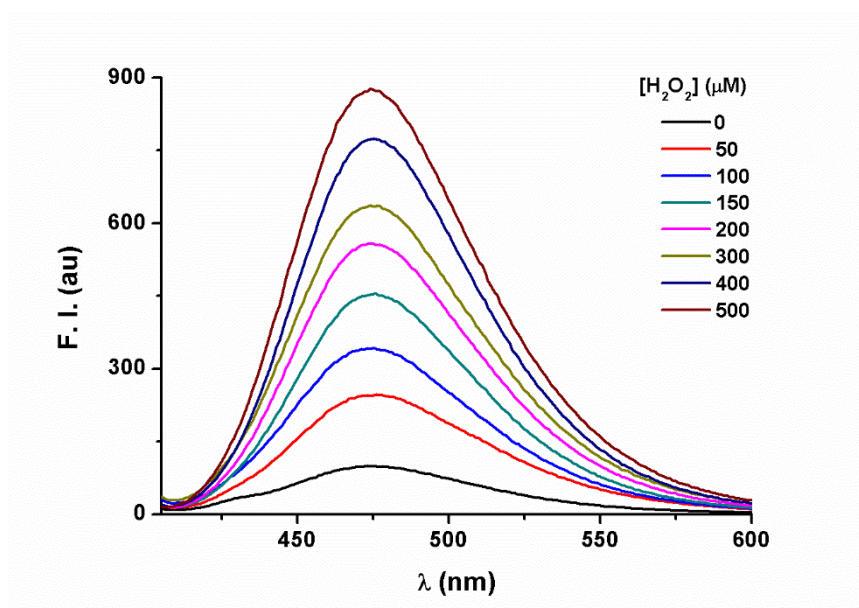
**Figure S3.** Fluorescence response of AP (10 μM) towards H<sub>2</sub>O<sub>2</sub> (400 μM) as time lapsed. Spectra were taken in PBS (pH 7.4, 100 mM) at 37 °C.



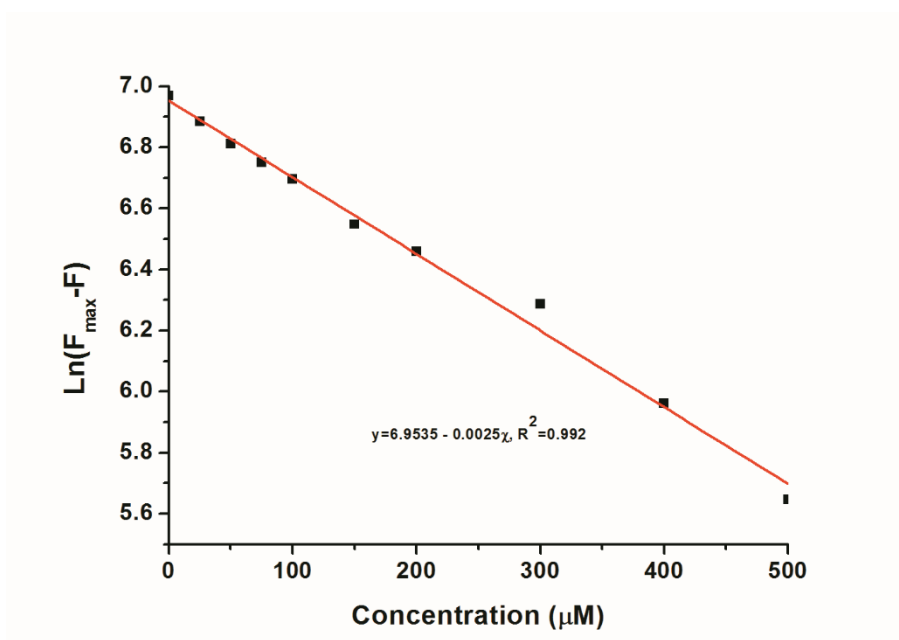
**Figure S4.** Fluorescence response of AP (10 μM) towards H<sub>2</sub>O<sub>2</sub> (500 μM) as time lapsed. Spectra were taken in PBS (pH 7.4, 100 mM) at 37 °C.



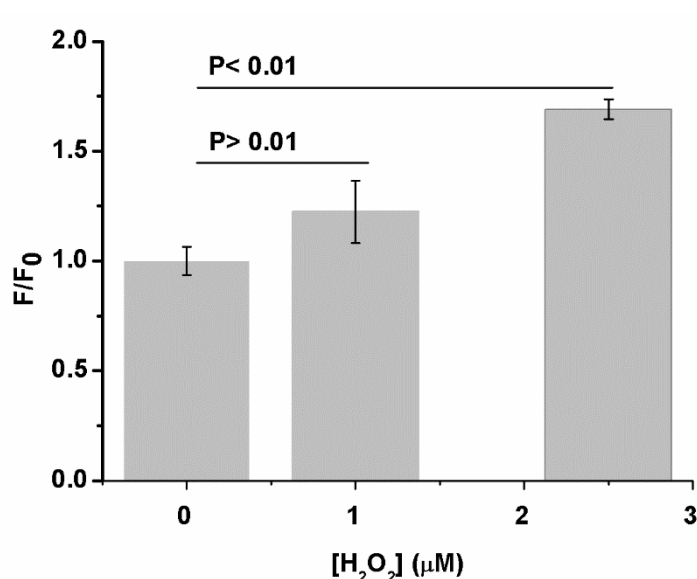
**Figure S5.** Fluorescence intensity of AP (10  $\mu\text{M}$ ) at 476 nm after the treatment of  $\text{H}_2\text{O}_2$  (200-600  $\mu\text{M}$ ) for various time. Data were taken in PBS (pH 7.4, 100 mM) at 37  $^\circ\text{C}$ .



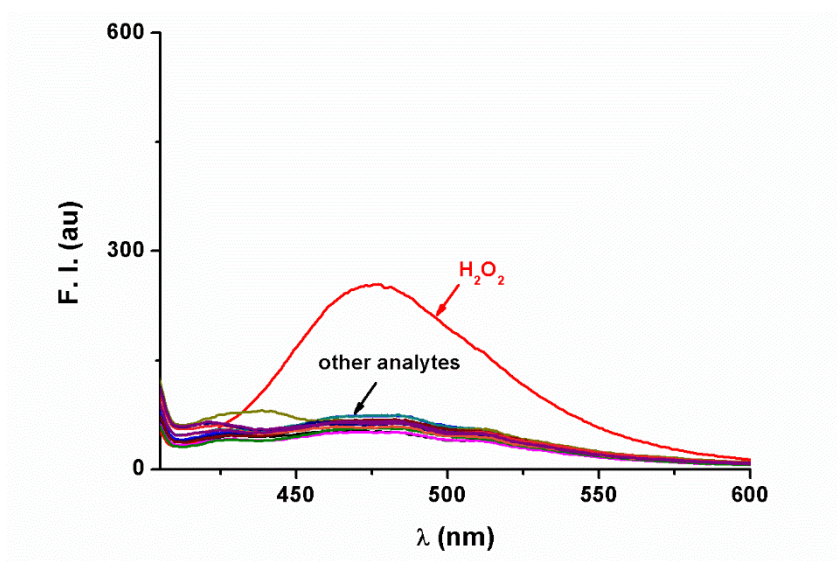
**Figure S6.**  $\text{H}_2\text{O}_2$  dose-dependent fluorescence enhancement of AP (10  $\mu\text{M}$ ). Spectra were taken in PBS (pH 7.4, 100 mM) at 37  $^\circ\text{C}$  after an incubation time of 60 min.



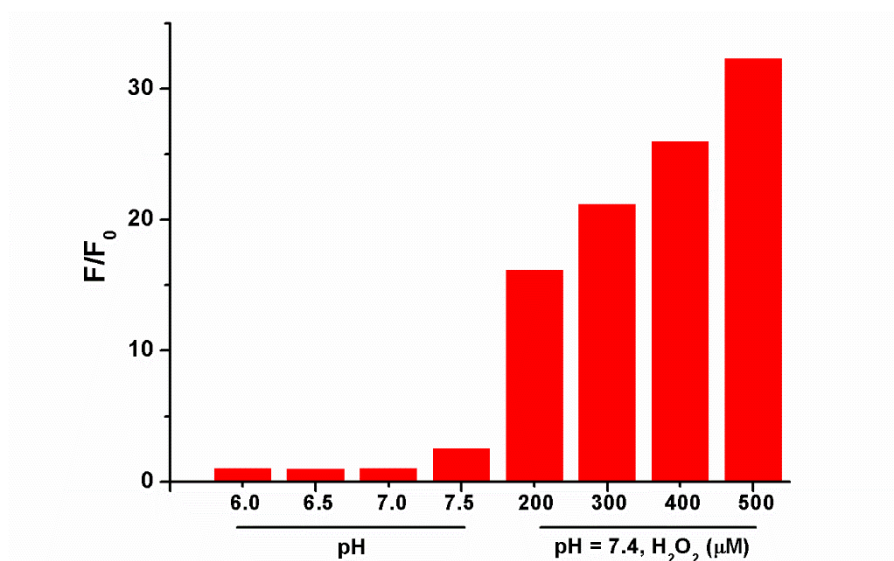
**Figure S7.** The Napierian logarithm of  $F_{\max}$  minus  $F$  correlated linearly with the corresponding  $\text{H}_2\text{O}_2$  concentrations (0 to 500  $\mu\text{M}$ ), and wherein  $F_{\max}$  is the maximum fluorescent intensity at 476 nm of **AP** after the treatment of a large enough amount of  $\text{H}_2\text{O}_2$ , and  $F$  is the fluorescence after the treatment of corresponding amount of  $\text{H}_2\text{O}_2$ . Data were acquired in the same way as those in Figure S5.



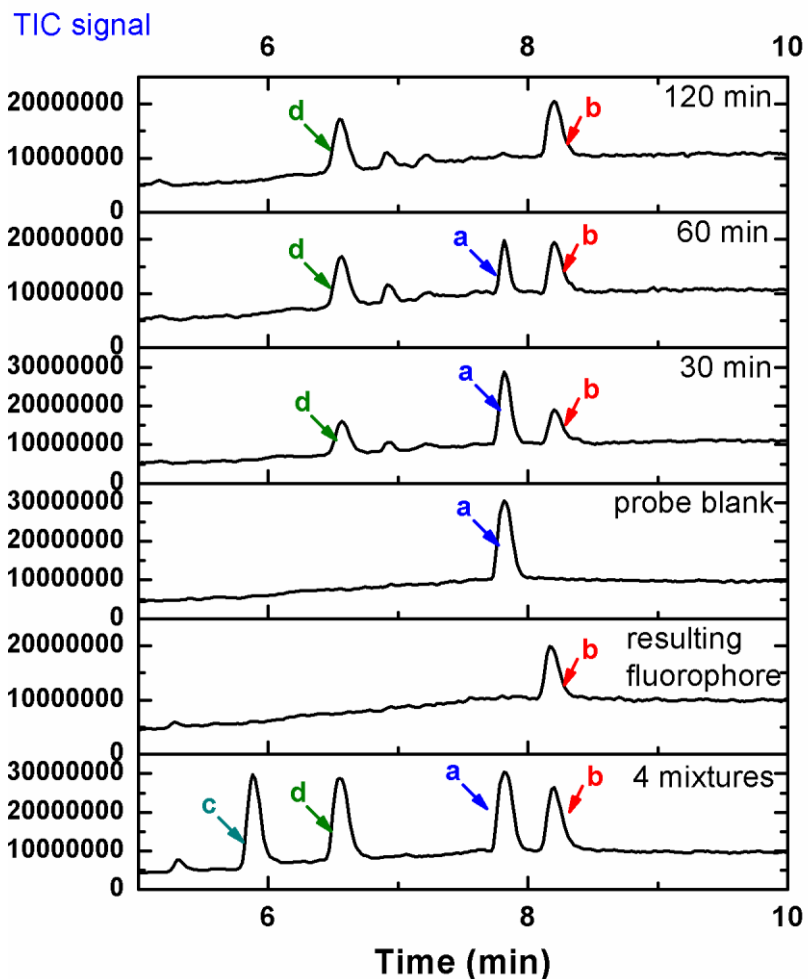
**Figure S8.** The detection limit determination of **AP**. Results were obtained as the concentration of  $\text{H}_2\text{O}_2$  that induced a statistically significant increase in fluorescence intensity at 476 nm compared with a blank control with a  $p$ -value  $< 0.01$ . Experiments were carried out by incubating **AP** (10  $\mu\text{M}$ ) with  $\text{H}_2\text{O}_2$  (0, 1.0, 2.5  $\mu\text{M}$ ) in PBS (100 mM, pH 7.4) at 37°C for 60 min and then collecting the emission at 476 nm by excitation at 375 nm.  $F$ : fluorescence intensity at 476 nm after treating **AP** with various concentrations of  $\text{H}_2\text{O}_2$ ;  $F_0$ : fluorescence intensity at 476 nm of probe blank control. Statistical analyses were performed with a two-tailed Student's  $t$ -test ( $n = 3$ ). Error bars are standard deviation.



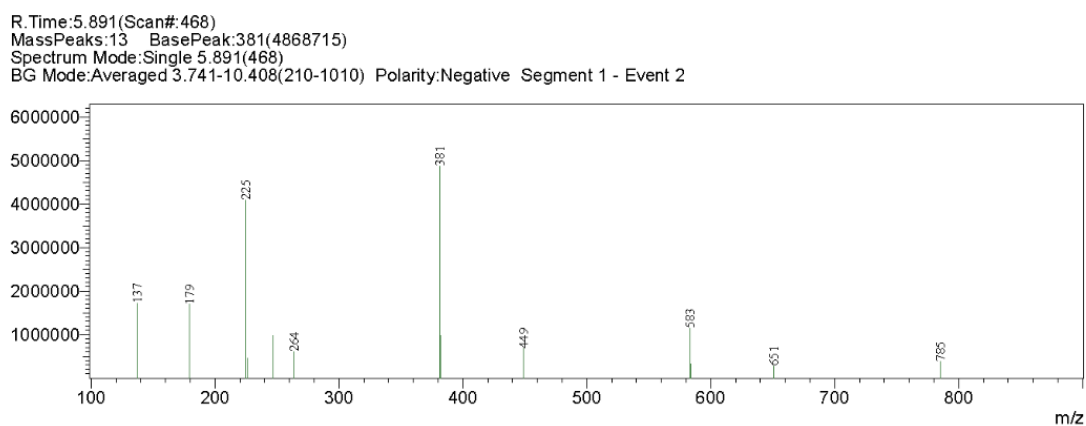
**Figure S9.** Fluorescent spectra of AP (10  $\mu\text{M}$ ) in the presence of various bio-relevant reactive species (200  $\mu\text{M}$ ). Spectra were taken in PBS (100 mM, pH 7.4) after an incubation time of 30 min at 37  $^{\circ}\text{C}$  with excitation 375 nm.



**Figure S10.** The effect of pH on AP stability indicated by fluorescence increase. Data shown were the fluorescence increase of AP (10  $\mu\text{M}$ ) at 476 nm after 30 min of incubation in PBS of indicated pH, or after being treated with H<sub>2</sub>O<sub>2</sub> of indicated concentration at pH 7.4. F<sub>0</sub> is the intensity of freshly prepared solutions at indicated pH.

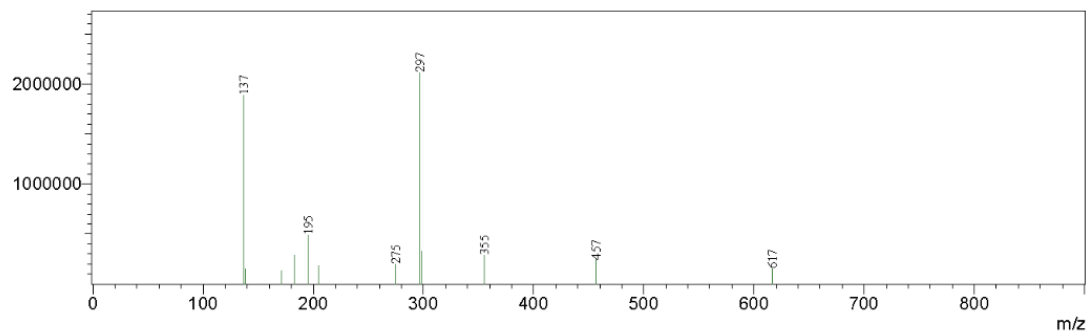


**Figure S11.** The total ion chromatogram (TIC) traces of probe AP (a), 2-(2'-hydroxy-4'-fluorophenyl) benzothiazole fluorophore (b), aspirin (c) and salicylic acid (d), and that of the detection reaction.



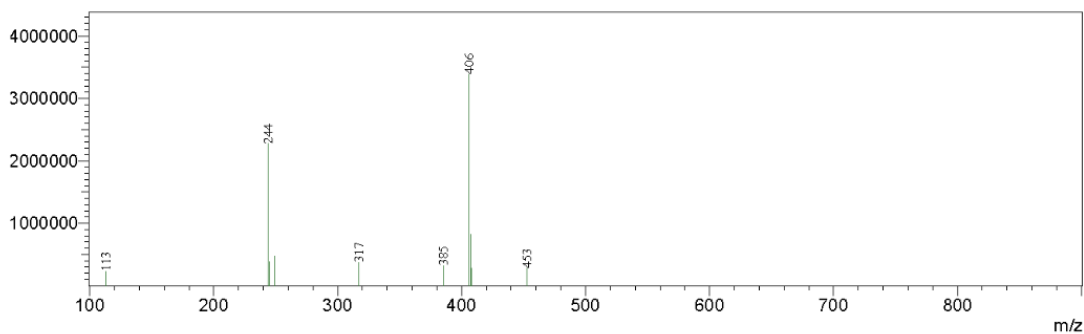
**Figure S12.** MS spectra of aspirin ( $m/z$  179 for  $[M-1]^{-1}$ ) (peak c).

R. Time: 6.558 (Scan#: 548)  
MassPeaks: 12 BasePeak: 297(2113946)  
Spectrum Mode: Single 6.558(548)  
BG Mode: Averaged 5.525-10.125(424-976) Polarity: Negative Segment 1 - Event 2



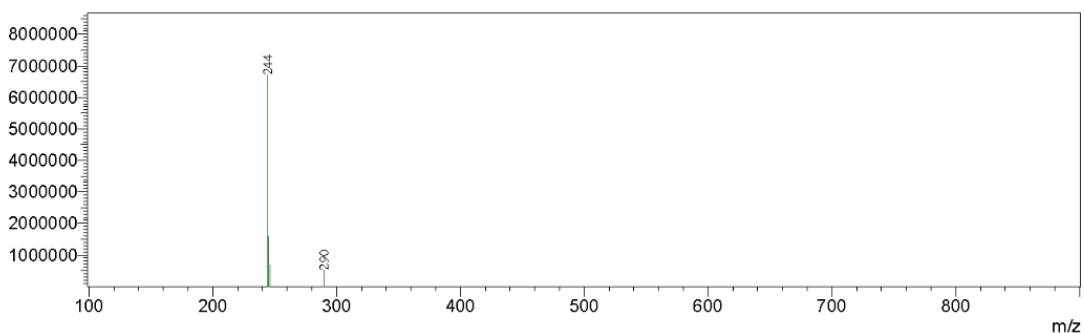
**Figure S13.** MS spectra of salicylic acid ( $m/z$  137 for  $[M-1]^{-1}$ ) (peak d).

R. Time: 7.825 (Scan#: 700)  
MassPeaks: 10 BasePeak: 406(3392718)  
Spectrum Mode: Single 7.825(700)  
BG Mode: Averaged 7.608-8.808(674-818) Polarity: Negative Segment 1 - Event 2

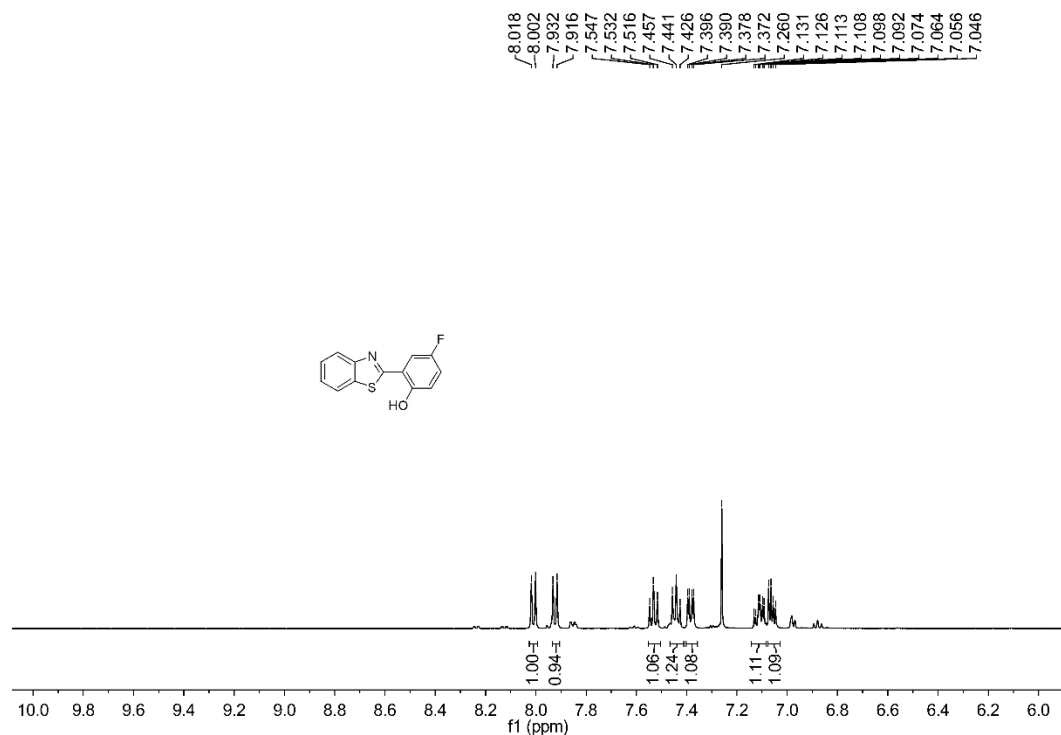


**Figure S14.** MS spectra of AP ( $m/z$  406 for  $[M-1]^{-1}$ ) (peak a).

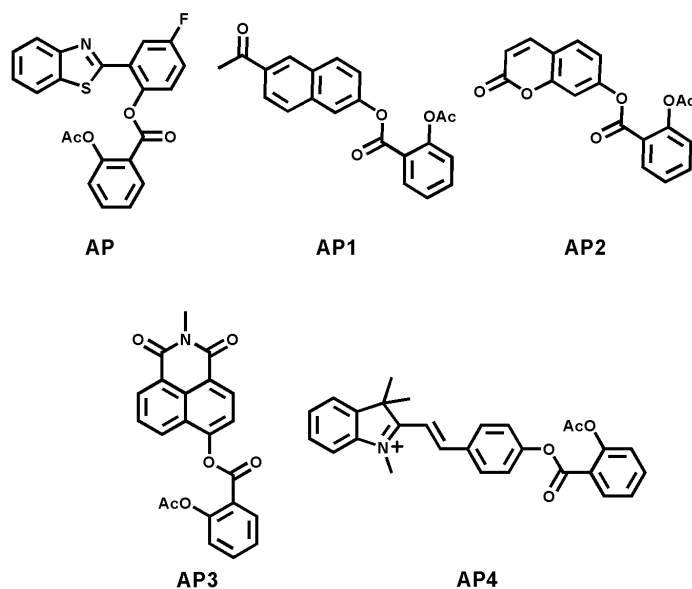
R. Time: 8.191 (Scan#: 744)  
MassPeaks: 4 BasePeak: 244(6715196)  
Spectrum Mode: Single 8.191(744)  
BG Mode: Averaged 4.808-12.058(338-1208) Polarity: Negative Segment 1 - Event 2



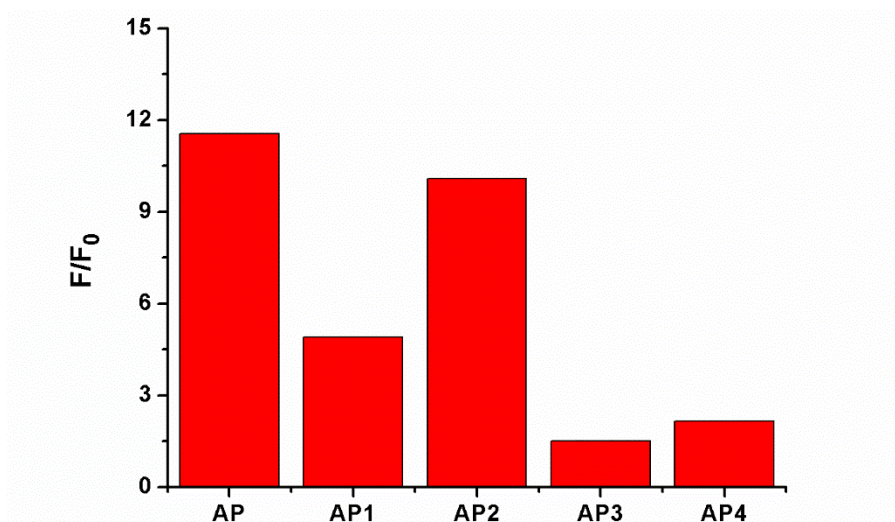
**Figure S15.** MS spectra of 2-(2'-hydroxy-4'-fluorophenyl) benzothiazole fluorophore ( $m/z$  244 for  $[M-1]^{-1}$ ) (peak b).



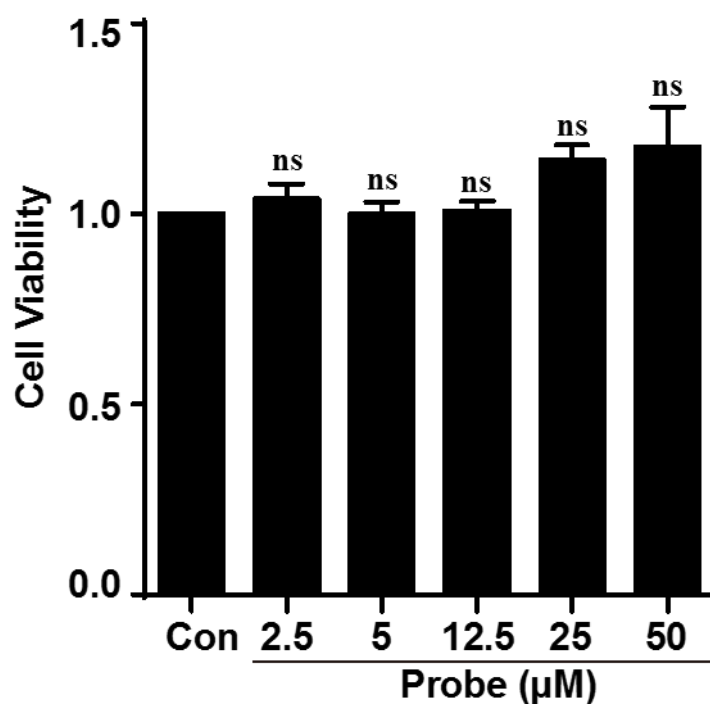
**Figure S16.**  $^1\text{H}$  NMR spectra of the fluorophore yielded in the detection reaction. **AP** was reacted with  $\text{H}_2\text{O}_2$  in a mixture of PBS and EtOH (1:1) at ambient temperature. The mixture was then extracted with EtOAc. After a quick wash with brine of the EtOAc phase, it was dried over anhydrous  $\text{Na}_2\text{SO}_4$ , evaporated and the residue characterized by  $^1\text{H}$  NMR.



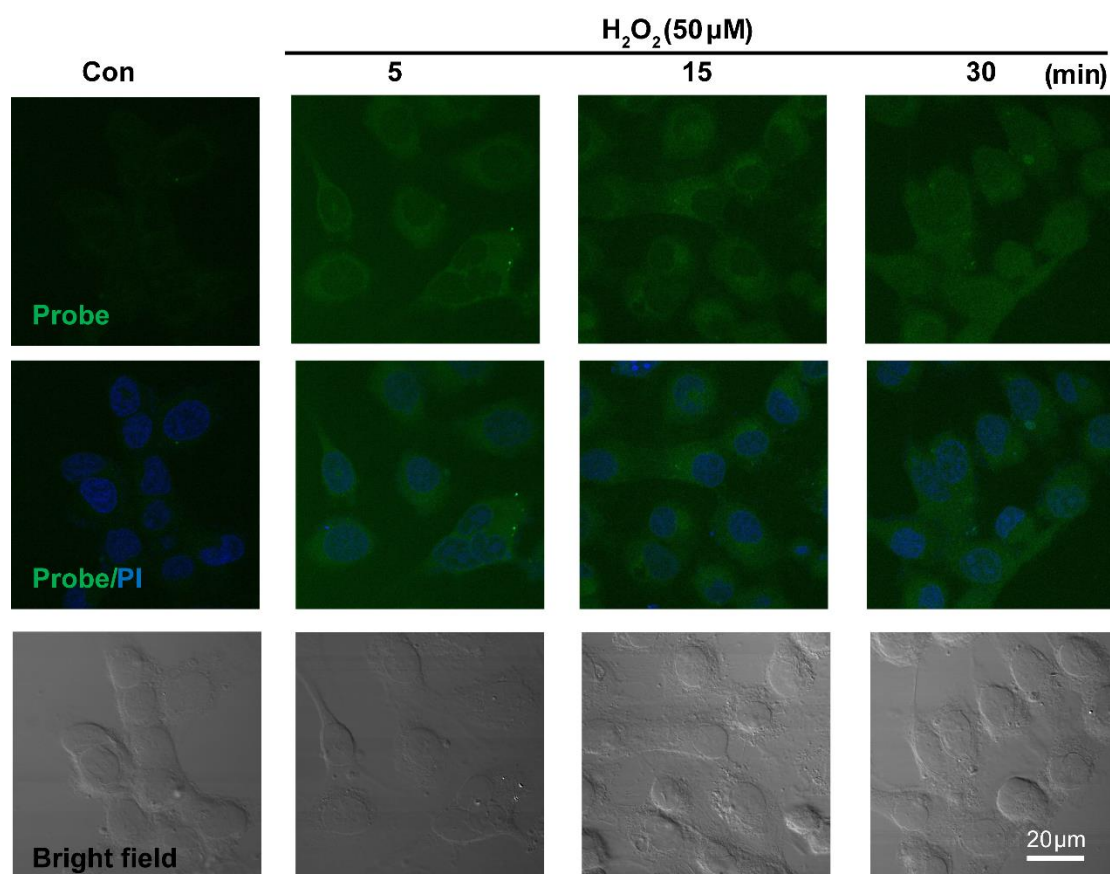
**Figure S17.** Structures of probe **AP1-AP4**.



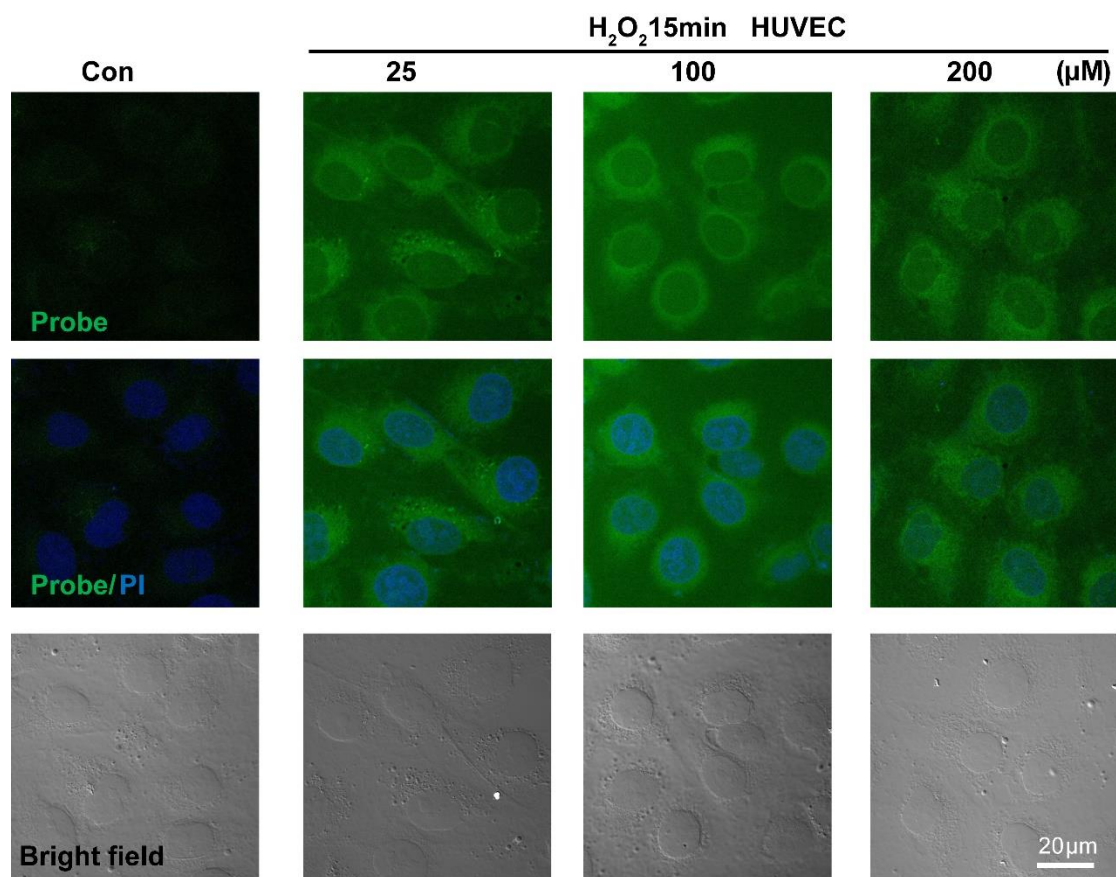
**Figure S18.** Fluorescent responses of probe **AP** or **AP1-AP4** towards H<sub>2</sub>O<sub>2</sub>. Probes (10 μM) were treated with H<sub>2</sub>O<sub>2</sub> (200 μM) for 30 min at 37°C in PBS (pH 7.4, 100 mM). Then the fluorescence increase in comparison to the freshly prepared probe solutions was recorded by a fluorescence spectrophotometer at 476 nm for **AP** (λ<sub>ex</sub> 375 nm), 431 nm for **AP1** (λ<sub>ex</sub> 324 nm), 455 nm for **AP2** (λ<sub>ex</sub> 324 nm), 551 nm for **AP3** (λ<sub>ex</sub> 374 nm), 553 nm for **AP4** (λ<sub>ex</sub> 517 nm).



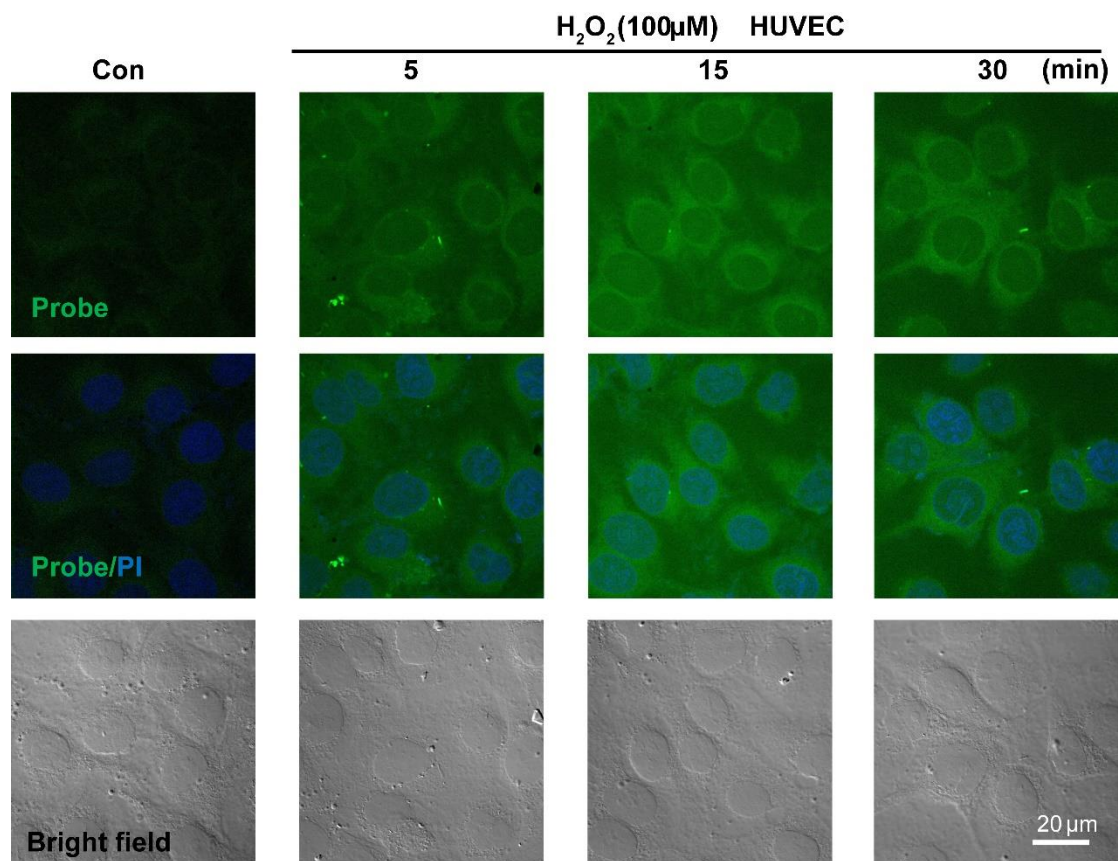
**Figure S19.** Mean cell viability under indicated conditions determined with a Cell Counting Kit-8 assay. EA.hy926 cells were treated with different concentrations of probe **AP** for 24 h, then CCK8 assay was used to check the cytotoxicity of **AP** probe. Ns, no significant changes.



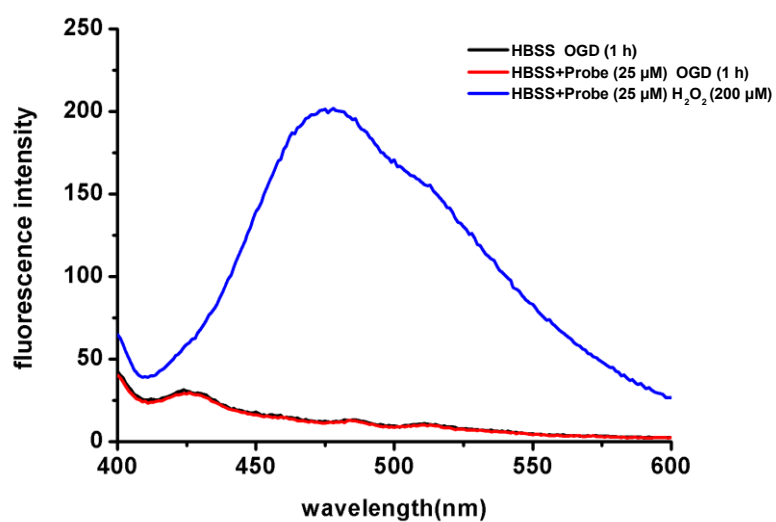
**Figure S20.** Representative confocal images of temporal increase of AP fluorescence in endothelial cells. The cells were seeded on 24-well glass cover slips overnight and then pre-incubated with AP (5.0 μM) for 15 min, followed by stimulation with or without H<sub>2</sub>O<sub>2</sub> (50 μM) for 5, 15, 30 min. PI counterstaining indicated nuclear localization (blue). All images were captured using a Nikon A1R confocal microscope. Overlay image of all captured fluorescence intensities are shown. Scale bar represents 20 μm.



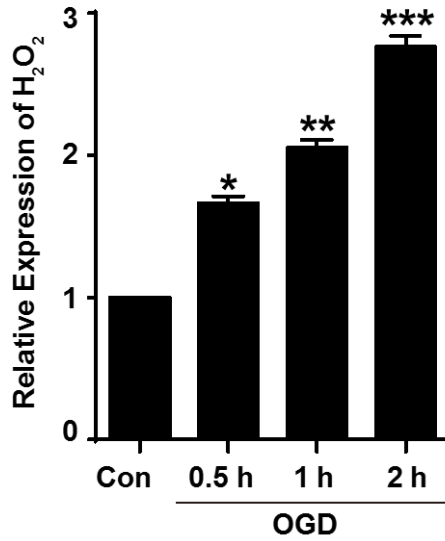
**Figure S21.** Confocal immunofluorescence images of probe **AP** were obtained from HUVEC cells following various concentrations of H<sub>2</sub>O<sub>2</sub> challenge. The cells were seeded on 24-well glass cover slips overnight and then pre-incubated with **AP** (5.0  $\mu$ M) for 15 min, followed by stimulation with or without H<sub>2</sub>O<sub>2</sub> (25-200  $\mu$ M) for 15 min. PI counterstaining indicated nuclear localization (blue). All images were captured using a Nikon A1R confocal microscope. Overlay image of all captured fluorescence intensities are shown. Scale bar represents 20  $\mu$ m.



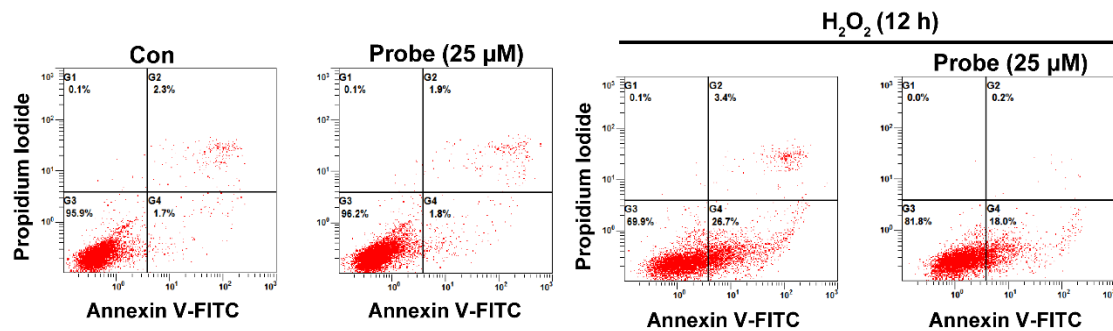
**Figure S22.** Representative confocal images of temporal increase of AP fluorescence in HUVEC cells. The cells were seeded on 24-well glass cover slips overnight and then pre-incubated with AP (5.0 μM) for 15 min, followed by stimulation with H<sub>2</sub>O<sub>2</sub> (100 μM) for indicated time. PI counterstaining indicated nuclear localization (blue). Overlay image of all captured fluorescence intensities are shown. Scale bar represents 20 μm.



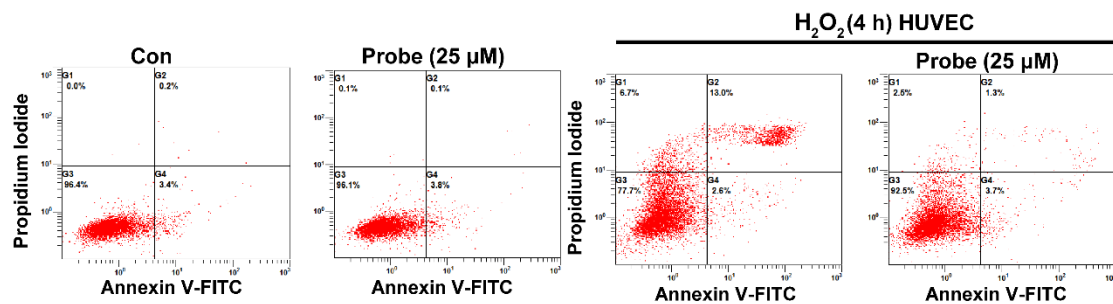
**Figure S23.** OGD agents caused no change to AP fluorescence.



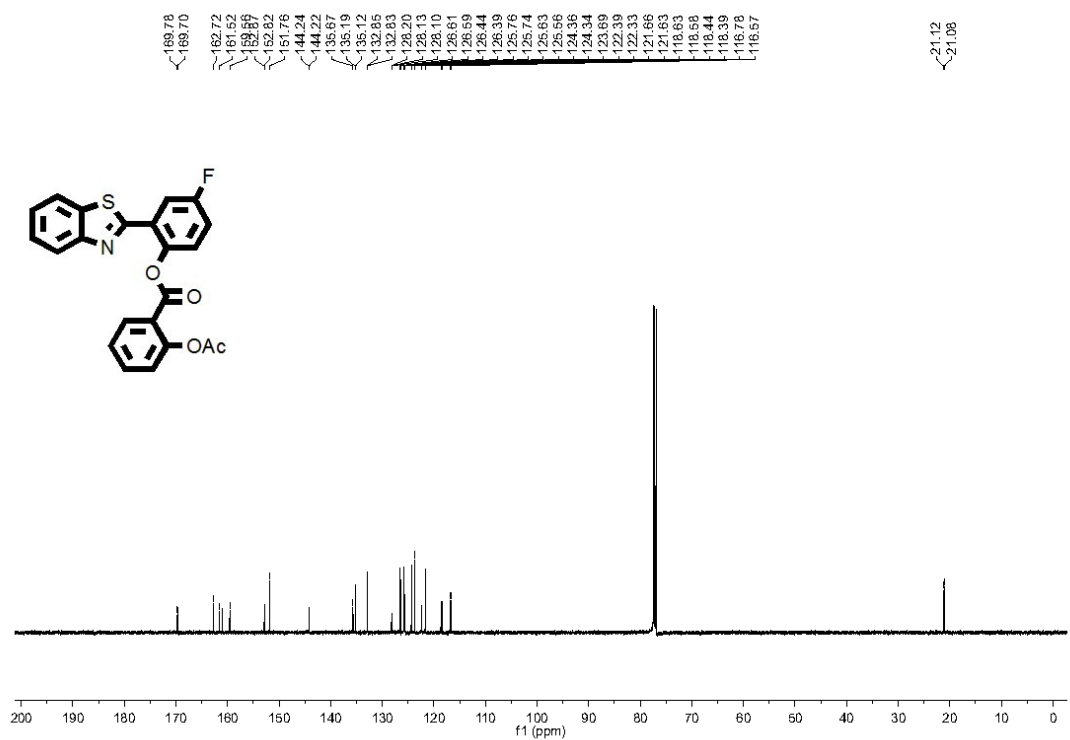
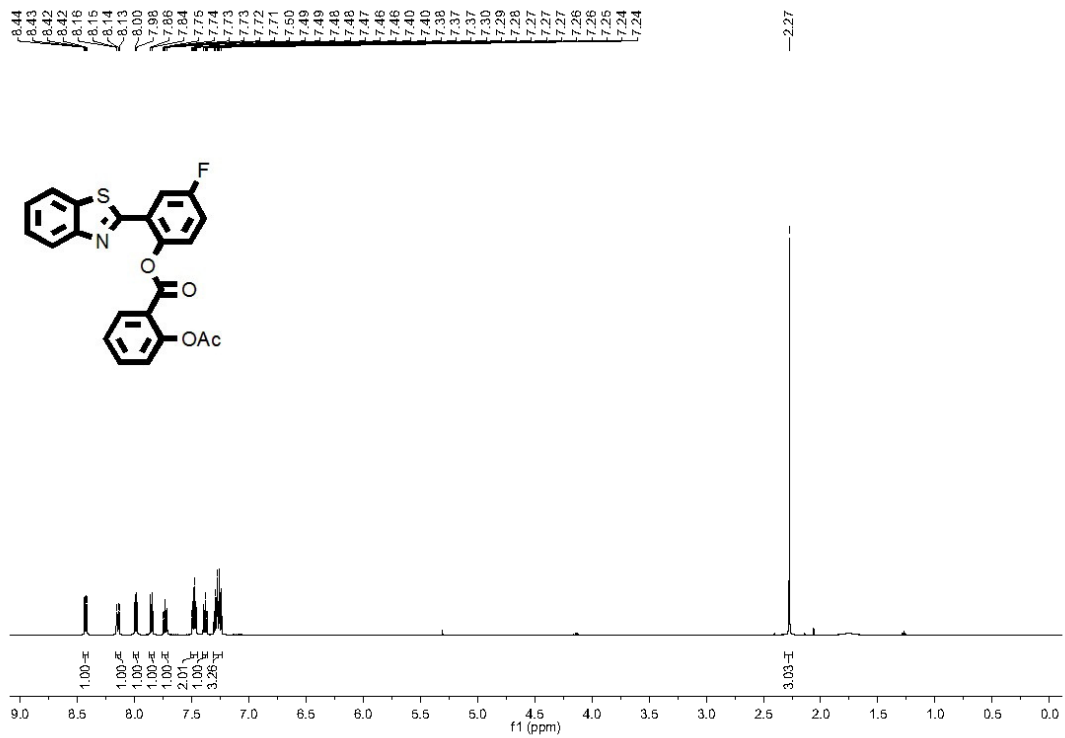
**Figure S24.** The intracellular H<sub>2</sub>O<sub>2</sub> levels were checked using a Hydrogen Peroxide Assay Kit (Beyotime Biotechnology) according to manufacturer instructions. Time-dependent accumulation of H<sub>2</sub>O<sub>2</sub> was observed in EA.hy926 cells over 0.5-2 h following OGD treatment.



**Figure S25.** Probe AP reduced H<sub>2</sub>O<sub>2</sub>-induced EA.hy926 endothelial apoptosis. The apoptosis of endothelial cells was determined using flow cytometry with annexin V-FITC/propidium iodide (PI). The EA.hy926 cells were seeded on 12-well plates overnight and then pre-incubated with AP (25.0 μM) for 15 min, followed by stimulation with H<sub>2</sub>O<sub>2</sub> (200 μM) for 12 h in DMEM medium.



**Figure S26.** The protective role of AP against H<sub>2</sub>O<sub>2</sub>-induced HUVEC apoptosis. The apoptosis of HUVEC cells was determined using flow cytometry with annexin V-FITC/propidium iodide (PI). The cells were seeded on 12-well plates overnight and then pre-incubated with AP (25 μM) for 15 min, followed by stimulation with H<sub>2</sub>O<sub>2</sub> (200 μM) for 4 h in HBSS medium.



NMR traces of AP